International Journal of Greenhouse Gas Control 69 (2018) 20–35

Contents lists available at ScienceDirect

International Journal of Greenhouse Gas Control

journal homepage: www.elsevier.com/locate/ijggc

Comparison of various configurations of the absorption-regeneration process using different solvents for the post-combustion CO_2 capture applied to cement plant flue gases

Lionel Dubois, Diane Thomas*

Chemical and Biochemical Process Engineering Unit, Faculty of Engineering, University of Mons, 20 Place du Parc, 7000 Mons, Belgium

ARTICLE INFO

Keywords:
Post-combustion CO_2 capture
Absorption-regeneration process configurations
Solvents comparison
Aspen Hysys™ simulation
Lean and rich vapor compression
Cement plant flue gases

ABSTRACT

Carbon Capture Utilization or Storage (CCUS) has gained widespread attention as an option for reducing CO_2 emissions from power plants but specific developments are still needed for the application to cement plants. More precisely, the post-combustion CO_2 capture process by absorption-regeneration is the more mature technology but its cost reduction is still necessary. The present study is focusing on Aspen Hysys™ simulations of different CO_2 capture process configurations (namely "Rich Solvent Recycle" (RSR), "Solvent Split Flow" (SSF), "Lean/Rich Vapor Compression" (L/RVC)) applied to the flue gas coming from the Norcem Brevik cement plant (taken as case study) and using three different solvents, namely: monoethanolamine (MEA), piperazine (PZ) and piperazine-methyldiethanolamine (MDEA) blend. For each configuration and solvent, different parametric studies were carried out in order to identify the operating conditions ($(L/G)_{vol.}$, split fraction, flash pressure variation, etc.) minimizing the solvent regeneration energy. Total equivalent thermodynamic works and utilities costs were also analyzed. It was shown that the configurations studied allow regeneration energy savings in the range 4–18%, LVC and RVC leading to the higher ones. As perspectives, other configurations and combination of configurations will be considered in order to further reduce the energy consumption of the process.

1. Introduction

Based on the report published by the International Energy Agency (IEA, 2013), Carbon Capture Utilization or Storage (CCUS) process chain is absolutely needed for an efficient reduction of the greenhouse gases from industrial plants and especially of carbon dioxide. Regarding more specifically the carbon capture technologies, several studies have already been carried out for their application to power plants and full scale installations are now under operation, such as for example at Boundary Dam (Saskatchewan, Canada) where the post-combustion absorption-regeneration process using amines based solvents is used as carbon capture technology. A lot of pilot units and demonstration plants are presented in (Idem et al., 2015). Nevertheless, another large CO_2 emitting sector which contributes to around 5% of the global CO_2 emissions and to 30% of the industrial emissions, namely the cement industry, still needs a lot of research studies and technical developments before implementing CCUS. In this context, the European Cement Research Academy (ECRA) and the University of Mons (UMONS) established in 2013 a new Academic Chair with the purpose of studying the applicability of Carbon Capture and its Reuse for its specific application in the cement industry where the CO_2 content of the gas to treat (namely between 17% and 35% depending on the plant) is higher than for power plant flue gases (typically between 5% and 15%). This Academic Chair is also supported by HeidelbergCement. Indeed, Norcem AS (HeidelbergCement Group) has joined forces with ECRA to establish a small-scale test centre for studying and comparing various post-combustion CO_2 capture technologies (namely amine scrubbing, membrane technology, solid adsorbent technology and carbonate looping process), and determining their suitability for implementation in modern cement kiln systems (Bjerge and Brevik, 2014). The project does not encompass CO_2 transport and storage. The small-scale test centre has been established at Norcem's cement plant in Brevik (Norway). This project launched in May 2013 has received funding from Gassnova through the CLIMIT program and it is scheduled to conclude in spring 2017.

Regarding more specifically the post-combustion CO_2 capture technology applying amines based absorption-regeneration process, the key point for allowing a large deployment of this technology is clearly its cost. In order to improve this process and to reduce its cost, three ways are possible. Firstly, the development of new solvents (new

* Corresponding author.
E-mail address: diane.thomas@umons.ac.be (D. Thomas).

https://doi.org/10.1016/j.ijggc.2017.12.004
Received 13 March 2017; Received in revised form 18 November 2017; Accepted 3 December 2017

Nomenclature

$\alpha_{CO2,rich/lean}$	CO_2 loading of the rich/lean solution (mol CO_2/mol amine)
A	Internal heat exchanger area (m^2)
CAPEX	Capital expenditure
$C_{utilities}$	Utilities costs (€/t_{CO2})
D	Column diameter (m)
$\Delta\alpha_{CO2}$	CO_2 cyclic capacity (mol CO_2/mol amine)
$\eta_{turbine}$	Power plant turbine efficiency (%)
$E_{condenser}$	Condenser cooling energy (GJ/t_{CO2})
E_{cooler}	Lean solvent cooling energy (GJ/t_{CO2})
$E_{LVC/RVC,compressor}$	Compressor energy consumption for the LVC/RVC configuration (GJ/t_{CO2})
E_{pumps}	Liquid pumps energy consumption (GJ/t_{CO2})
E_{regen}	Specific solvent regeneration energy (GJ/t_{CO2})
G	Gas flow rate (m^3/h)
$G_{CO2,produced}$	Rate of CO_2 generated at the stripper's top (t_{CO2}/h)
H	Column height (m)
ICA	Inter-Cooled absorber configuration
L	Liquid flow rate (m^3/h)
$L_{lean,opt}$	Optimum liquid flow rate of the lean solution (m^3/h)
LVC	Lean vapor compression configuration
MDEA	Methyldiethanolamine
MEA	Monoethanolamine
OPEX	Operational expenditure
P_{bottom}	Pressure at the bottom of the column (kPa)
Φ_{boiler}	Heat duty at the stripper's bottom (GJ/h)
RSR	Rich Solvent Recycle configuration
RVC	Rich vapor compression configuration
SSF	Solvent split flow configuration
T_C	Steam condensation temperature in the power plant turbine (°C)
T_H	Steam temperature in the reboiler
$T_{liquid,in}$	Liquid temperature at the inlet of the column (°C)
T_{regen}	Regeneration temperature at the stripper's bottom (°C)
$T_{rich,preheat}$	Rich solution temperature at the internal heat exchanger's outlet (°C)
U	Heat transfer coefficient (kJ/h m^2 °C)
W_{equ}	Total equivalent thermodynamic work (GJ/t_{CO2})
y_{CO2}	CO_2 content of the gas phase (vol.%)

solutions or new blends) with high absorption capacity while keeping good absorption kinetics allows to reduce significantly the solvent regeneration energy. An example is given in the works of (Singh et al., 2013) showing that new solvents have the potential to reduce the reboiler energy requirements by 20–50% in comparison with a 31 wt% MEA solution as reference solvent. Secondly, implementing more efficient equipment such as new gas-liquid contactors or new packings leads to an improvement of the absorption performances, which allows the solvents to reach a CO_2 loading which is close to its maximum absorption capacity while reducing the OPEX and CAPEX of the process. The works of (Zhao et al., 2011) show that the use of new packing elements leads to higher mass transfer coefficients (increase of around 25%) when compared to conventional Mellapak 700Y and 13 mm Pall Ring, allowing a lower packed column height. Finally, the third way to improve the global performances of the absorption-regeneration technology is implementing new process configurations in order to take advantage of a better energy integration and to reduce its energy consumption. (Le Moullec et al., 2014) give more details regarding the technical description and the interest of other process configurations.

The present paper focuses on this third possibility and especially on the regeneration cost savings linked to the implementation of advanced process configurations for a flue gas issued from a cement plant. The flue gas coming from Norcem Brevik Cement plant was considered and the CO_2 capture pilot simulated in Aspen Hysys™ software was based on the installation used during the CASTOR/CESAR European Projects (Knudsen et al., 2009), all the design and operating parameters being available in order to validate the simulation. The configurations considered are described in Section 2.3 and the solvents selected in our study are: monoethanolamine (MEA), piperazine (PZ) and piperazine-methlydiethanolamine (MDEA) blend.

Table 1
Reactions included in the Acid Gas Package for MEA, PZ and MDEA solvents reacting with CO_2.

Category	N°	Reaction	Type
Water related			
	(1)	$2\,H_2O \leftrightarrow H_3O^+ + OH^-$	Equilibrium
	(2)	$H_2O + HCO_3^- \leftrightarrow H_3O^+ + CO_3^{2-}$	Equilibrium
	(3)	$CO_2 + OH^- \rightarrow HCO_3^-$	Kinetic
	(4)	$HCO_3^- \rightarrow CO_2 + OH^-$	Kinetic
MEA related			
$(HO(CH_2)_2NH_2)$	(5)	$HO(CH_2)_2H^+NH_2 + H_2O \leftrightarrow HO(CH_2)_2NH_2 + H_3O^+$	Equilibrium
	(6)	$HO(CH_2)_2NH_2 + H_2O + CO_2 \rightarrow HO(CH_2)_2NHCOO^- + H_3O^+$	Kinetic
	(7)	$HO(CH_2)_2NHCOO^- + H_3O + \rightarrow HO(CH_2)_2NH_2 + H_2O + CO_2$	Kinetic
PZ related			
$(C4H8(NH)_2)$	(8)	$C_4H_8(NH)_2 + H_3O^+ \leftrightarrow C_4H_8(NH)_2H^+ + H_2O$	Equilibrium
	(9)	$C_4H_8(NH)_2HCOO + H_2O \leftrightarrow C_4H_8(NH)_2COO^- + H_3O^+$	Equilibrium
	(10)	$C_4H_8(NH)_2 + H_2O + CO_2 \rightarrow C_4H_8(NH)NCOO^- + H_3O^+$	Kinetic
	(11)	$C_4H_8(NH)NCOO^- + H_3O^+ \rightarrow C_4H_8(NH)_2 + H_2O + CO_2$	Kinetic
	(12)	$C_4H_8(NH)NCOO^- + H_2O + CO_2 \rightarrow C_4H_8(NCOO^-)_2 + H_3O^+$	Kinetic
	(13)	$C_4H_8(NCOO^-)_2 + H_3O^+ \rightarrow C_4H_8(NH)NCOO^- + H_2O + CO_2$	Kinetic
MDEA related			
$(CH_3N(CH_2CH_2OH)_2)$	(14)	$CH_3N(CH_2CH_2OH)_2 + H_3O^+ \leftrightarrow CH_3N(CH_2CH_2OH)_2H^+ + H_2O$	Equilibrium
	(15)	$CH_3N(CH_2CH_2OH)_2 + H_2O + CO_2 \rightarrow CH_3N(CH_2CH_2OH)_2H^+ + HCO_3^-$	Kinetic
	(16)	$CH_3N(CH_2CH_2OH)_2H^+ + HCO_3^- \rightarrow CH_3N(CH_2CH_2OH)_2 + H_2O + CO_2$	Kinetic

2. Simulation of different process configurations

2.1. Aspen Hysys™ modeling parameters

The modeling was developed in Aspen Hysys™ v.8.6 software using the Acid Gas Package and the "Efficiency calculation mode". The Acid Gas Package developed by Aspen allows to simulate the removal of acid gases as CO_2 and H_2S. It includes the physicochemical properties of these acid gases, water, amines alone (such as MEA and PZ) and also several mixtures (such as MDEA + PZ), a rate-based calculation model and a makeup unit operation to compensate losses in water and amine in the system. The Acid Gas Property Package is based on extensive research and development in rate-based, chemical absorption process simulation and molecular thermodynamic models for aqueous amine solutions (Zhang et al., 2009). More specifically, the thermodynamic models used in the Acid Gas property package are the Electrolyte Non-Random Two-Liquid (eNRTL) activity coefficient model for electrolyte thermodynamics in liquid phase (Song and Chen, 2009) and the Peng-Robinson equation of state for the vapor phase. The property package contains the eNRTL model parameters and other transport property model parameters identified from regression of extensive thermodynamic and physical property data for aqueous amine solutions (Zhang and Chen, 2011; Zhang et al., 2011).

The reactions included in the Acid Gas Package are listed in Table 1. In addition to the dissociation reactions (reactions (1)–(4)) considered for all the solvents, specific reactions are added depending on the solvent selected for the simulation. In the case of PZ-MDEA blend, reactions related to both solvents are taken into account in the calculations.

Regarding the calculation mode, two rate-based models are available in Aspen Hysys for the simulation of the absorber and regenerator units, namely "Efficiency" and "Advanced Modeling". The Advanced model uses Maxwell-Stefan theory to rigorously calculate the heat and mass-transfer rates without assuming thermal or chemical equilibrium between the vapor and liquid for each stage. The Efficiency model uses in a first step a conventional equilibrium-stage model to solve the column, but the non-equilibrium behavior inherent in acid gas systems is modeled in a second step by calculating a rate-based efficiency for CO_2 at each stage. The results from the Efficiency and Advanced models are comparable for most systems and the Advanced model is recommended when significant quantities of other specific gaseous contaminants are present in the gas to treat and must be rigorously simulated. Therefore, the Efficiency calculation mode was selected in the present work as it has been checked that the results obtained with the two models were similar while Efficiency modeling converges much faster than the Advanced one.

2.2. Operating and design conditions – description of the conventional process configuration

The flowsheet developed in Aspen Hysys™ is illustrated on Fig. 1 for the conventional process configuration.

Table 2
Dimensions and operating conditions of the columns.

	Absorber	Stripper
D (m)	1.1	1.1
H (m)	17 (17 × 1 m)	10 (10 × 1 m)
Packing	Random packing IMTP 50	Random packing IMTP 50
$T_{liquid,in}$ (°C)	40	110
P_{bottom} (kPa)	120	200

The CASTOR/CESAR pilot unit was selected as case study because all the design and operating parameters are available in literature, which is not the case with most of the other installations. The pilot is sized to handle a flow of 5000 Nm^3/h (at the inlet of the treatment line). This results in a flow of around 4000 m^3/h at the inlet of the absorption column after excess water removal, cooling and compression.

Two important simulation parameters are imposed: the absorption ratio, equal to 90% (90% of the molar flow rate of CO_2 entering the absorption column is recovered at the outlet of the regeneration column); and the produced CO_2 purity, fixed at 98 mol% (conventional specification).

The dimensions of the absorber and the stripper, and the operating conditions for each column are also set (see Table 2).

Thanks to the internal heat exchanger the temperature of the liquid at the inlet of the stripper is fixed at 110 °C as base case (corresponding to a pinch of around 10 °C at the hot side of the exchanger). In addition, the linear pressure drop per unit height in the absorber and the stripper are fixed to 0.5 kPa/m.

The flue gas coming from the Norcem Brevik Cement plant in Norway (average values of gaseous composition) was taken as a representative example. The flue gas leaves the cement plant at 165 °C and 100 kPa. It is compressed to an absolute pressure of 120 kPa and cooled down to 40 °C before entering the flow sheet on Fig. 1. The conditioned gas ("gas to treat", ≈4000 m^3/h, see composition in Table 3) is sent in the absorber where the CO_2 is captured by an amine-based solvent.

The CO_2 content of the gas to treat (y_{CO2}) was therefore equal to around 20% for all the simulations but the specific impact of y_{CO2} on the absorption-regeneration performances will be illustrated in Section 4.5 but is also discussed in another paper (Dubois et al., 2017).

The amount of CO_2 absorbed into the column is calculated using the "rate-based model". At the outlet of the column, the solution is pumped and preheated to 110 °C thanks to the internal heat exchanger. Then, in the regeneration column, the gas is stripped thanks to the heating power and the CO_2 is recovered at the top of the regeneration column. The regeneration occurs at 200 kPa and at the solvent boiling point (for example around 120 °C for an aqueous MEA 30 wt.% solution at such pressure level). The condenser cooling energy is automatically adjusted in order to satisfy the CO_2 purity specification. The regenerated solvent which still contains some CO_2 is pumped through the heat exchanger in

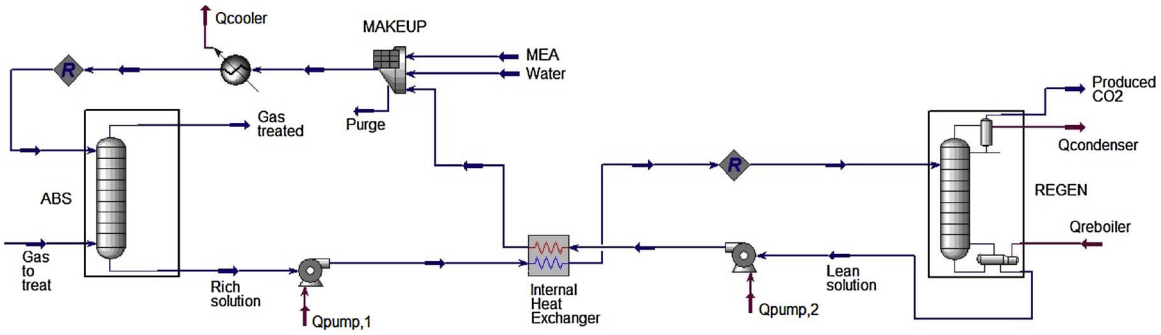

Fig. 1. Aspen Hysys™ flow sheet for the conventional process configuration (illustration for MEA).

Table 3
Composition of the gas to treat (G = 3997 m^3/h, 40 °C, 120 kPa) after conditioning.

Component	mol frac.
N_2	64.7%
CO_2	20.4%
H_2O	6.2%
O_2	8.6%
CO	1330 ppm
SO_2	111 ppm
NO	474 ppm
NO_2	2 ppm

order to be cooled down. To compensate possible losses in amine and water at the outlet of the absorber and the regenerator, a makeup unit is added in order to automatically adjust the total flow of liquid while reaching the desired concentration of amine. Note that as this makeup unit ensures the water and solvent balance, the washing section situated at the top of the absorber in the real installation was not simulated in the present work as it does not influence the absorption-regeneration global performances. After this make up unit, the lean solution is cooled down to 40 °C before entering the absorption column and beginning a new absorption-regeneration cycle.

2.3. Types of process configuration improvements considered

As indicated previously, many process configurations and the technical details associated are given in (Le Moullec et al., 2014). Three categories of process improvements are envisaged. First of all the absorption enhancement modification whose purpose is to increase the CO_2 loading at the absorber bottom. In the present case, the "Rich Solvent Recycle" (RSR) configuration (see Fig. 2) was considered.

The principle of this configuration is to recycle into the absorber a part of the rich solution coming from the bottom of this column. The rich solution going back to the column can also be cooled down in order to promote the CO_2 absorption. In addition to the liquid flow rate (liquid to gas ratio, L/G) that must be optimized for all the configurations, the other parameters that must be specifically adjusted for RSR configuration in order to minimize the energy consumption of the system (especially the solvent regeneration energy) are: the fraction of the rich solution recycled, the temperature of the solution before reinjection into the column and the level of reinjection into this column.

The second modification envisaged is the exergetic (or heat) integration. The general idea of these process modifications is to perform heat integration between the different process streams in order to reduce the heat losses and the solvent regeneration energy. The process modification corresponding to this category and considered in the present case is the "Solvent Split Flow" (SSF) configuration (see Fig. 3), also called "Rich Solvent Splitting". With this configuration, a part of the rich solution coming from the absorber is directly sent at the top of the regeneration column without being preheated by the internal heat exchanger. This arrangement leads to a modification of the temperature profile into the stripper (it is more smoothed than with conventional configuration) and the heat integration inside the process is improved. Indeed, the hot stream coming from the stripper will transmit his energy to a smaller rich solvent flow rate, leading to a slightly higher solvent temperature at the top of the stripper and reducing the temperature difference between the solvent inlet temperature and the boiler regeneration temperature which is favourable for the regeneration process (decrease of the sensible heat part in the regeneration energy). Furthermore, thanks to the cold solution injected at the top of the stripper, the condenser cooling energy is reduced.

The parameters that must specifically optimized for SSF configuration are: the fraction of the cold rich solution by-passing the internal heat exchanger and the injection levels of the solutions (cold rich solution and preheated rich solution) into the stripper.

Moreover, for a defined heat exchanger, splitting the rich solution with SSF will change the liquid flow rate inside this exchanger leading to a modification of the temperature of the rich solution at its outlet ($T_{rich,preheat}$) (equal to 110 °C in the base case with MEA 30 wt.%). As used for example in (Sanchez Fernandez et al., 2012), the internal heat exchanger was simulated using the product "UA [kJ/°C h]" of the heat

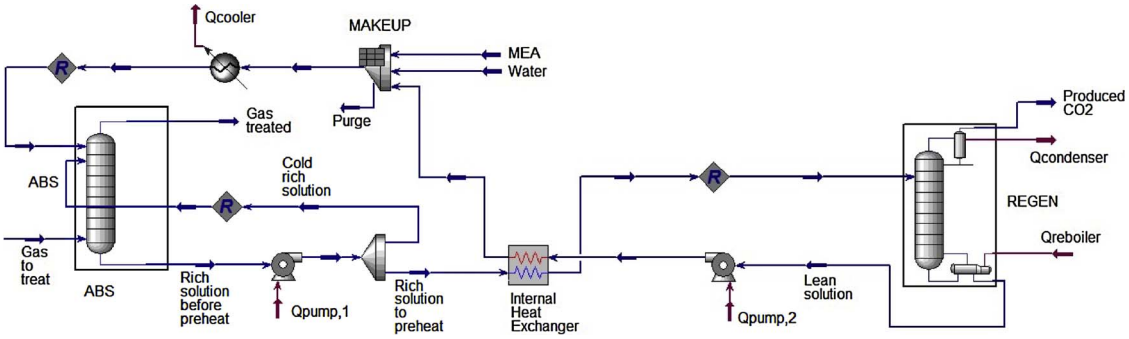

Fig. 2. Aspen Hysys™ flow sheet for the Rich Solvent Recycle (RSR) process configuration (illustration for MEA).

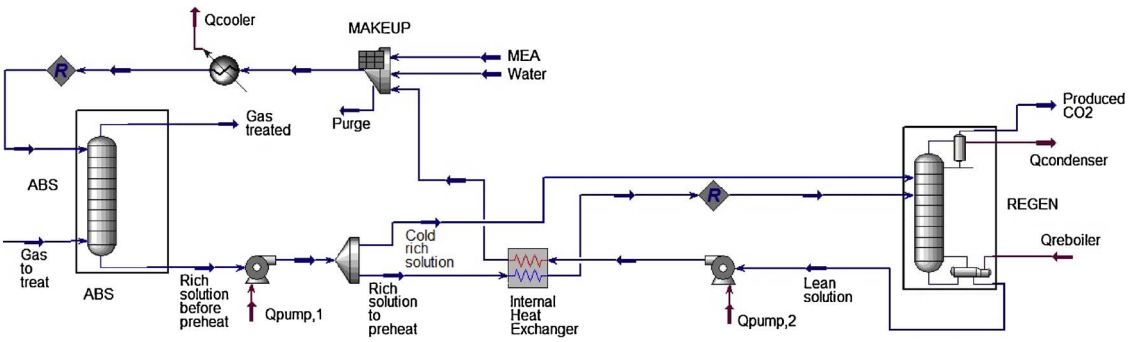

Fig. 3. Aspen Hysys™ flow sheet for the Solvent Split Flow (SSF) process configuration (illustration for MEA).

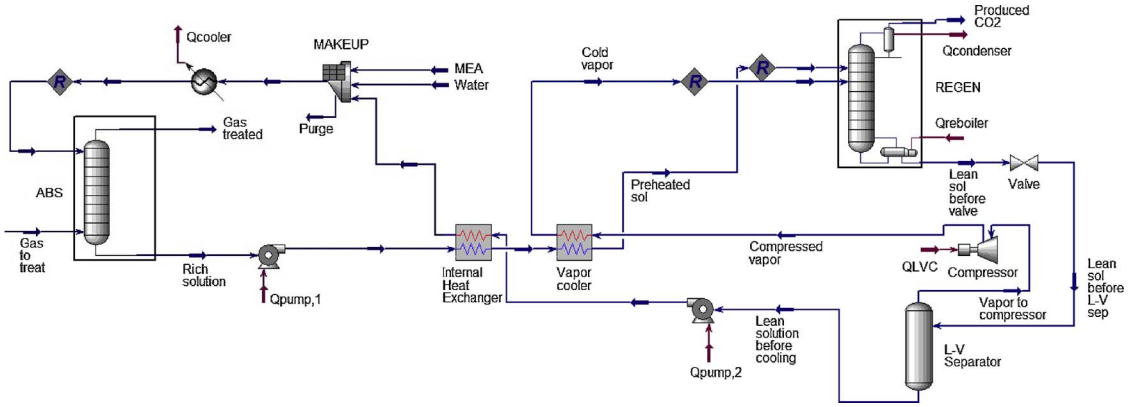

Fig. 4. Aspen Hysys™ flow sheet for the Lean Vapor Compression (LVC) process configuration (illustration for MEA).

transfer coefficient (U [kJ/h m^2 °C]) and area (A [m^2]) corresponding to the base case. Based on the same principle, using the UA parameter coming from the base case configuration (without SSF), simulations were performed for different liquid flow rate values at the inlet of the internal heat exchanger in order to establish the relation between this flow rate and the temperature at the outlet of the internal heat exchanger ($T_{rich,preheat}$).

The third category of process modifications is based on a heat pump effect. The idea of this process modification category is to increase the heat quality provided to the system. As described by (Le Moullec et al., 2014), this effect enables the valorization of heat available at a too low quality level or, more generally, when increasing the quality level is profitable. Two configurations corresponding to this category are considered in the present study, namely the "Lean Vapor Compression" (LVC) (see Fig. 4) and the "Rich Vapor Compression" (RVC) (see Fig. 5).

The principle of the LVC configuration is as follows: the lean solvent at the bottom of the stripper is flashed in order to produce a gaseous stream (mainly composed of water and carbon dioxide) which is compressed and fed back to the stripper. Such process modification reduces the reboiler steam demand and cools down the lean solvent going to the internal heat exchanger. Furthermore, the lean solvent exits the flash tank at lower temperature and heats the rich solvent in the heat exchanger also to a lower temperature, making the top of the stripper a bit colder which reduces the cooling requirement in the condenser. Based on operational experiences such as in the CASTOR/CESAR project (Knudsen et al., 2009), this modification is generally accompanied with an expansion or a modification of the internal heat exchanger in order to reduce the hot pinch of this exchanger to 5 °C.

Indeed, even if injecting the rich solvent into the stripper at a lower temperature is beneficial in terms of condenser cooling energy, it is counterbalanced by an unfavorable larger temperature difference between the inlet liquid temperature and the boiling temperature. Moreover, as the vapor coming from the compressor installed after the flash unit is very hot (which could lead to a hot spot inducing degradation problems into the bottom of the stripper), a supplementary internal heat exchanger can be installed in order to cool down this vapor (to 120 °C) while giving a preheating complement to the rich solution before entering the regeneration column.

Regarding the "Rich Vapor Compression" (RVC) configuration, the principle is quite similar as the LVC one even if it is the hot rich solvent which is flashed instead of the lean solution in order to produce a gaseous stream sent into the bottom of the stripper. As for LVC configuration, an expansion of the internal heat exchanger or a supplementary heat exchanger can be installed in order to cool down the vapor stream to 120 °C (for MEA) and to give a supplementary preheating to the rich solution before its regeneration.

In addition to the liquid flow rate, the important operating parameter in relation with LVC and RVC configurations is the flash pressure variation (Δp). This pressure variation depends on the stripper pressure but it has to be noted that a too low pressure (under atmospheric one) is not advised for economic reasons.

As a conclusion of this section, it must be noted that four different

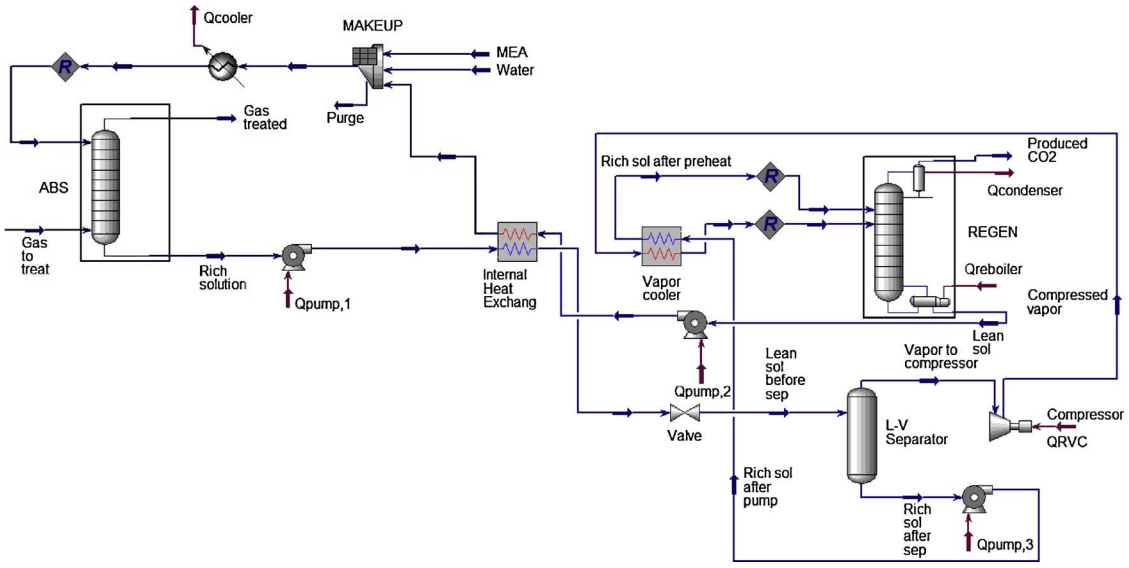

Fig. 5. Aspen Hysys™ flow sheet for the Rich Vapor Compression (RVC) process configuration (illustration for MEA).

Table 4
Specific operating conditions adopted for each solvent.

Amine(s)	Amine(s) concentrations (wt.%)	Absorber pressure (kPa)	Stripper pressure (kPa)
MEA	30	120	200
PZ	40	120	200–600
PZ + MDEA	40 (varying proportions)	120	600

configurations are considered in the present work, namely RSR, SSF, LVC and RVC, corresponding to the three categories of process modifications. The focus is put to these configurations because it does not imply too many modifications of the conventional process and some of them (such as LVC) have already shown interesting results for the application to power plants which have to be confirmed for the application to cement plants.

2.4. Specific operating parameters adopted for each solvent

As already stated, the selected solvents in this study are: monoethanolamine (MEA), piperazine (PZ) and piperazine-methlydiethanolamine (MDEA) blend. The specific operating conditions (amine(s) concentration(s), absorber pressure and stripper pressure) adopted for each solvent in the simulations are summarized in Table 4.

Regarding the primary amine MEA, the conventional solvent concentration is 30 wt.% and as this solvent was used in the industrial pilot installation simulated, no adaptations of the operating conditions were necessary.

Concerning the cyclic diamine PZ, it can be used both alone or blended with another solvent. Based on (van der Ham et al., 2014) and (Freeman et al., 2010), PZ is conventionally used with a concentration of 40 wt.% (8 M). Therefore, this concentration was considered in the simulations. Moreover, even if in a first step, the simulations were carried out with the same design and operating parameters as for MEA 30 wt.%, in a second step, as PZ-based solvents are generally regenerated at high temperature, the influence of the reboiler pressure was studied. Indeed, the PZ 40 wt.% (8 M) regeneration process is generally carried out under pressure and with a boiler temperature of 150 °C (the absorption temperature being equal to 40 °C indicating that the absorption occurs to a pressure close to the atmospheric one). Thus, simulation results were compared considering different pressure levels from 200 kPa (as for MEA 30 wt.%) to 600 kPa (final pressure value kept for the performances comparisons with other solvents).

Finally, for the PZ-MDEA blend, such as considered e.g. in (Mudhasakul et al., 2013) and (Roh et al., 2016), the total amine concentration of the solvent used in the CO_2 capture process is around 50 wt.% (different proportions between PZ and MDEA are possible) and with pressure of 25–40 bar and 2–5 bar for the absorption and regeneration respectively. Nevertheless, in the present case, in order to make "realistic comparisons" between the three solvents considered (MEA, PZ and PZ-MDEA), the simulations were carried out with the same design and operating parameters as for PZ 40 wt.% (such as the pressure in the columns, fixed at 120 kPa and 600 kPa for the absorption and regeneration respectively). The total amine concentration was also limited to 40 wt.% but the "optimum" PZ/MDEA proportion was defined during preliminary simulations.

3. Simulation results obtained with the conventional process configuration

Before analyzing the results, it must be noted that the simulation method was previously validated with the use of CASTOR/CESAR projects results (application to power plant) and also with the use of another study (other pilot design but same modeling method) concerning the application to a cement plant (see (Gervasi et al., 2014) for more details).

Concerning the methodology used in this work, as described in the exergetic and exergoeconomic analysis of (Ferrara et al., 2017), the main part (around 65%) of the irreversibilities being associated to the stripping column and especially to the reboiler duty, the objective of the present study was to minimize the specific solvent regeneration energy (E_{regen} [GJ/t_{CO2}]) defined as:

$$E_{regen} = \frac{\Phi_{boiler}}{G_{CO_2,produced}} \quad (17)$$

where Φ_{boiler} [GJ/h] is the heat duty provided at the bottom of the stripper and $G_{CO2,produced}$ [t_{CO2}/h] the rate of CO_2 generated at the top of this column (outlet of the condenser). Note that no compression of the produced CO_2 is considered in the present case because in accordance with ECRA (European Cement Research Academy) the focus is put on CO_2 valorization options for which the level of CO_2 compression can be different depending on the CO_2 conversion process considered.

As some configurations imply the optimization of several operating parameters, systematic parametric studies were carried out in order to identify the realistic conditions leading to the minimum of E_{regen}. Firstly, each operating parameter was varied separately and secondly, cross variations were carried out in order to identify the operating parameters minimizing E_{regen}.

Even if the focus was put on minimizing E_{regen}, two other indicators were also analyzed, namely the total equivalent thermodynamic work (W_{equ} [GJ/t_{CO2}]) and the total utilities costs ($C_{utilities}$ [€/t_{CO2}]).

W_{equ} was calculated based on the method described in (Karimi et al., 2011):

$$W_{equ} = E_{regen}\left(1 - \frac{T_C + 273.15}{T_H + 273.15}\right)\eta_{turbine} + E_{pumps} + E_{LVC/RVC,compressor} \quad (18)$$

where T_C [°C] is the steam condensation temperature in the turbine of the power plant providing the electrical energy to the cement plant (assumed to be equal to 40 °C), T_H [°C] is the steam temperature in the reboiler (assumed to be 10 °C higher than the reboiler temperature T_{regen}), $\eta_{turbine}$ is the turbine efficiency (assumed to be equal to 75%), E_{pumps} and $E_{LVC/RVC,compressor}$ [GJ/t_{CO2}] the electrical energies used to run the pumps and the compressor with LVC or RVC configuration. Indeed, such approach allows to unify the thermal and electrical energy consumptions, the thermal regeneration energy being converted to electrical energy by calculating how much electricity can be produced with the same amount of steam for the reboiler.

Concerning $C_{utilities}$ [€/t_{CO2}], it is provided by Aspen Economics module available in Aspen Hysys and considering the software default parameters for the economic calculations (e.g. plant location in North America, 2013 as construction year, engineering procurement construction (EPC) duration of 20 weeks, etc.). These utilities costs include the electricity, the cooling water and the steam costs. The advantage of such indicator is to combine the different types of energy consumptions (such as W_{equ}) but also to consider the cooling water costs. W_{equ} and $C_{utilities}$ values are provided in Section 4.5.

3.1. Conventional configuration with MEA

3.1.1. Optimization of the liquid to gas flow rate ratio

For the absorption-regeneration CO_2 capture process, it is conventional to optimize the $(L/G)_{vol.}$ in order to minimize the regeneration energy. The simulated results for different $(L/G)_{vol.}$ (which means different liquid flow rates due to the fact that the gaseous flow rate was kept constant) are presented on Fig. 6.

First of all, it must be observed that the trend of this graph is quite typical for such process. The minimum regeneration energy was identified for a liquid flow rate of 22 m^3/h ($(L/G)_{vol.}$ = 5.56 10^{-3}) leading to E_{regen} = 3.36 GJ/t_{CO2}. This value is in the range of conventional

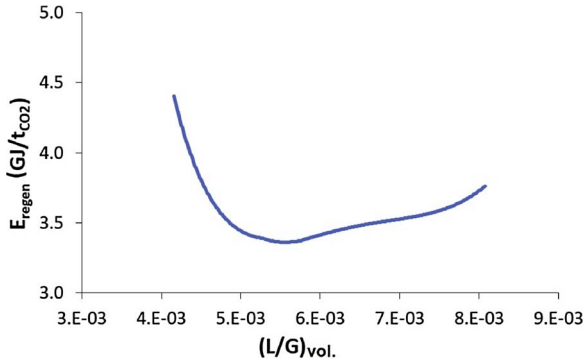

Fig. 6. Regeneration energy as a function of the $(L/G)_{vol.}$ ratio.

values measured for power plants (between 3 and 4 GJ/t_{CO2}, see for example (Knudsen et al., 2009)). Nevertheless, it must be pointed out that 3.36 GJ/t_{CO2} is close to the minimum values conventionally measured for MEA 30 wt.% which could be justified by the fact that a higher CO_2 content in the gas to treat (20 vol.% for the cement plant considered in the present case in comparison with the range 5–15 vol.% for power plants) is favourable to the absorption process.

3.1.2. Global results analysis for the conventional process configuration

The detailed results corresponding to the optimal operating conditions for the conventional process configuration are presented in Fig. 7., Tables 5 and 6 .

Regarding the temperature profiles into the absorber and stripper presented on Fig. 7., first of all it must be specified that the temperature mentioned for stage 17 of the absorber corresponds to the temperature of the inlet liquid (40 °C) and that the temperature for stage 0 of the stripper corresponds to the reboiler temperature (121.8 °C). The profiles are quite conventional for such operation units even if the maximum temperature reached into the absorber (around 85 °C) is a little bit higher than other values (75–80 °C) generally measured. This is linked to the higher CO_2 content of the gas to treat (20 mol% for the cement plant considered) in comparison with power plants (5–15 mol%) which induces a higher heat of reaction.

Table 5
Simulation results for the base case with MEA 30 wt.% ($(L/G)_{vol.} = 5.56\ 10^{-3}$).

Parameter	Value
E_{regen}	3.36 GJ/t_{CO2}
$E_{condenser}$	−1.90 GJ/t_{CO2}
E_{pumps}	$1.57\ 10^{-2}$ GJ/t_{CO2}
$\alpha_{CO2,rich}$	0.506 mol CO_2/mol MEA
$\alpha_{CO2,lean}$	0.211 mol CO_2/mol MEA

Table 6
Gaseous compositions in mol. fraction for the base case with MEA 30 wt.% ($(L/G)_{vol.} = 5.56\ 10^{-3}$).

Component	Gas treated	Produced CO_2
N_2	62.9%	154 ppm
CO_2	2.1%	98.0%
H_2O	26.4%	1.9%
O_2	8.3%	37 ppm
CO	1300 ppm	0.4 ppm
SO_2	54 ppm	298 ppm
NO	461 ppm	4 ppm
NO_2	0.4 ppm	7 ppm
MEA	377 ppm	80 ppm

Concerning the other parameters indicated in Table 5, in addition to the regeneration energy commented in the previous section, it can be seen that even if it is not an issue for the absorption-regeneration process, the condenser cooling energy ($E_{condenser}$) is significant (−1.90 GJ/t_{CO2}) and reducing it thanks to the use of alternative configurations would be also benefic in practice (reduction of the water flow rate circulating into the condenser). Regarding the consumption of the liquid pumps (E_{pumps}) equal to $1.57\ 10^{-2}$ GJ/t_{CO2}, it corresponds to only ≈0.5% of the regeneration energy and it is thus not significant for the evaluation of the overall energy consumption of the process.

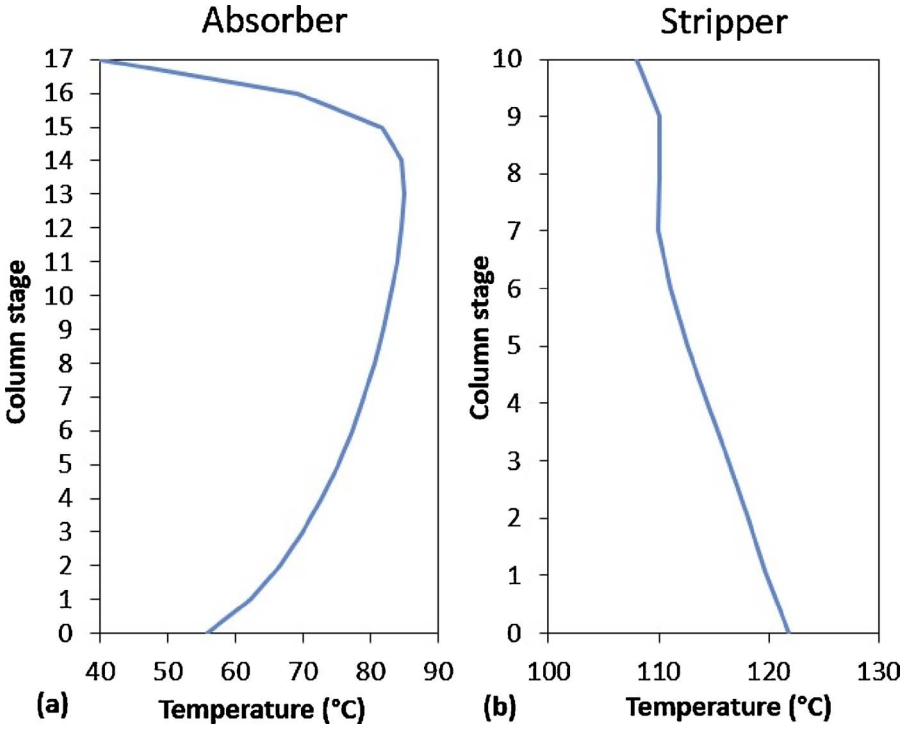

Fig. 7. Temperature profiles into the absorber (a) and the stripper (b).

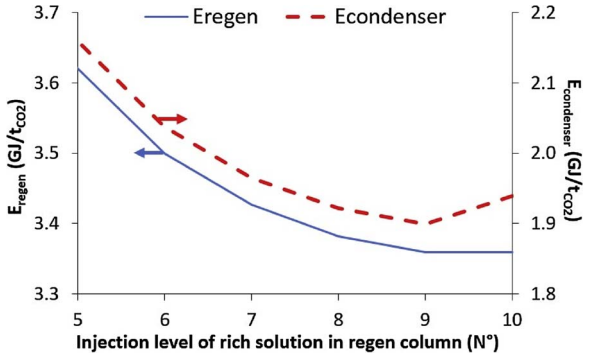

Fig. 8. E_{regen} and $E_{condenser}$ as a function of the injection of the rich solution into the stripper.

Moreover, the CO_2 loading values for the rich ($\alpha_{CO2,rich}$, at the outlet of the absorber) and the lean ($\alpha_{CO2,lean}$, at the outlet of the stripper) solutions are equal respectively to 0.506 and 0.211 mol CO_2/mol MEA, quite typical values for MEA 30 wt.% even if it must be noted that the value slightly higher than 0.5 is possible thanks to the CO_2 content of the gas to treat (≈ 20 mol%). Table 6 presents the gaseous compositions of the gas treated and the produced CO_2.

As no specific reactions were added concerning the other gaseous species (SO_2, NO, NO_2, etc.), the decrease of their concentrations into the absorber can only be associated to their solubilization into the liquid phase, and therefore the solvent degradation due to the presence of these gaseous contaminants are not part of the present work. Regarding the MEA, small quantities are present into the treated gas and the produced CO_2.

Note that in the real installation, the MEA quantity into the treated gas will be lower thanks to a water wash section (not simulated in the present case).

Finally, it has to be noticed that the presented results were obtained for a rich solution injected at stage N°9 into the stripper. Indeed, as presented on Fig. 8, injecting at stage N°9 or N°10 (top of the column) gives similar results in terms of regeneration energy while the condenser cooling energy is a little bit lower when the rich solution is not injected too close to the condenser, namely at stage N°9.

3.2. Conventional configuration with PZ

3.2.1. Influence of the regeneration pressure on the simulation results

As indicated in the previous section, PZ 40 wt.% (8 M) regeneration process is generally carried out under pressure and with a boiler temperature of 150 °C while the regeneration pressure considered for MEA 30 wt.% was 200 kPa. Therefore, simulations were carried out considering different pressure levels in the regeneration column, from 200 kPa (as for MEA 30 wt.%) to 600 kPa. It was inferred from our simulations that the boiler temperature of 150 °C was reached for a boiler pressure higher than 450 kPa.

Regarding the simulation results in terms of E_{regen}, Fig. 9 (a) shows the evolution of E_{regen} as a function of the $(L/G)_{vol.}$ for different boiler pressure values. It can be seen that increasing the boiler pressure allows to reduce the specific solvent regeneration energy. For example, the increase of the boiler pressure from 200 kPa to 600 kPa leads to a decrease of 25% of the regeneration energy (value for the $(L/G)_{vol.}$ minimizing E_{regen}, which is also reduced when the boiler pressure is increased). For each boiler pressure, Fig. 9(b) presents the optimal values of the specific solvent regeneration energy (E_{regen} minimized as a function of $(L/G)_{vol.}$).

Considering the boiler pressure leading to T_{regen} = 150 °C (namely 450 kPa), E_{regen} is equal to 3.36 GJ/t_{CO2} (same value as for MEA 30 wt.%) which means a decrease of almost 20% in comparison with the value obtained for the conventional configuration at 200 kPa (namely 4.19 GJ/t_{CO2}).

Finally, Fig. 10 shows the evolution of the CO_2 loadings (a) and of the optimum liquid flow rate (b) as a function of the boiler pressure.

It can be seen (Fig. 10(a)) that the increase of the boiler pressure leads to an increase of the rich solution loading and to a decrease of the lean solution loading. Therefore, as the CO_2 cyclic capacity ($\Delta\alpha_{CO2} = \alpha_{CO2,rich} - \alpha_{CO2,lean}$) is increasing, the optimum liquid flow rate value (Fig. 10(b)) is decreasing at higher pressure because the amount of CO_2 absorbed (L $\Delta\alpha_{CO2}$) is fixed as simulation parameter (90% of the absorber inlet CO_2 is recovered at the top of the stripper with 98 mol% purity). More precisely, increasing the boiler pressure leads to a higher regeneration temperature and to a better solvent regeneration. Due to this, the $\alpha_{CO2,lean}$ value is lower and leads to a better absorption in the absorption column (with the consequence of a higher $\alpha_{CO2,rich}$). To reach the same amount of CO_2 absorbed, as $\Delta\alpha_{CO2}$ will be

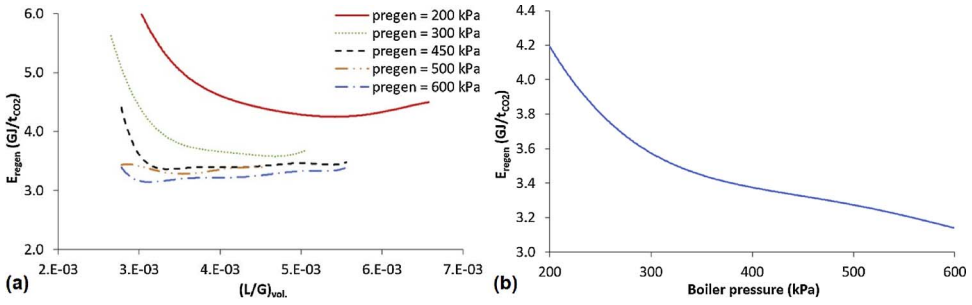

Fig. 9. E_{regen} as a function of the $(L/G)_{vol.}$ ratio for different boiler pressures (a) and E_{regen} value for the optimum $(L/G)_{vol.}$ ratio (b) – Conventional configuration with PZ 40 wt.%.

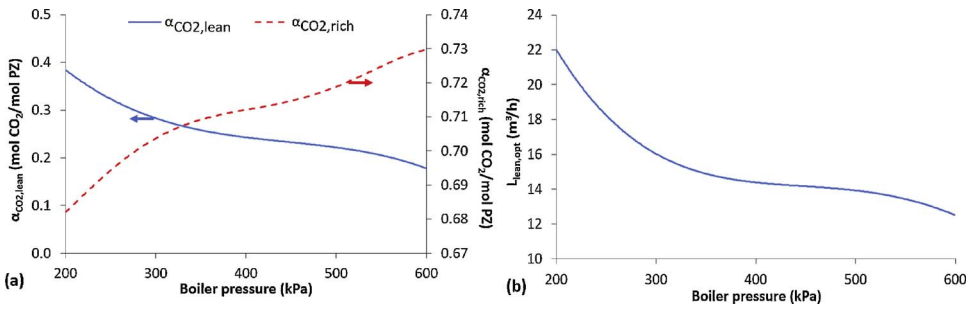

Fig. 10. CO_2 loadings of the rich and lean solutions (a) and optimum values of the liquid flow rate as a function of the boiler pressure (b) – Conventional configuration with PZ 40 wt.%.

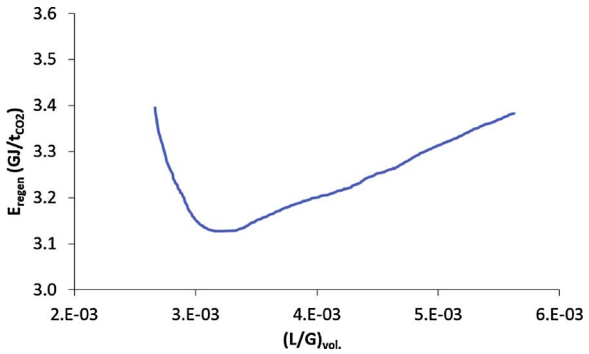

Fig. 11. Regeneration energy as a function of the $(L/G)_{vol.}$ ratio (PZ 40 wt.%, P_{boiler} = 600 kPa).

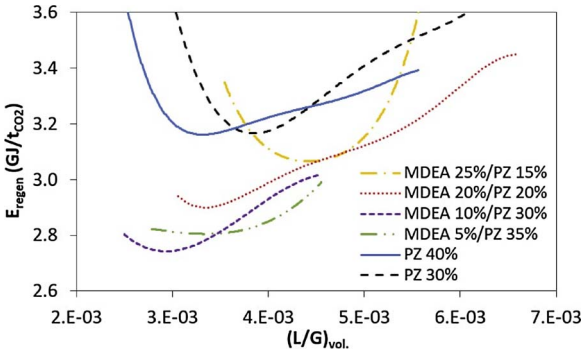

Fig. 12. Regeneration energy as a function of the $(L/G)_{vol.}$ for different MDEA/PZ proportions in PZ + MDEA solvent.

higher, the liquid flow rate will be decreased to reach the same capture rate.

3.2.2. Detailed simulation results considering a regeneration pressure of 600 kPa

As for MEA 30 wt.%, Fig. 11 presents the evolution of E_{regen} as a function of $(L/G)_{vol.}$ focusing on the results obtained for a regeneration pressure of 600 kPa. It can be seen that E_{regen} is minimized at $(L/G)_{vol.}$ equal to 3.16 10^{-3}, corresponding to a liquid flow rate of 12.5 m^3/h. Note that at such stripper pressure, T_{boiler} is equal to 161 °C. The detailed results are given in Table 7. Considering the optimum value of L, E_{regen} is equal to 3.14 GJ/t_{CO2} which means 6.5% energy savings in comparison with the base case of MEA 30 wt.% (3.36 GJ/t_{CO2}). Concerning the other parameters indicated in Table 7 in addition to the regeneration energy, it can be seen that the condenser cooling energy ($E_{condenser}$) is lower (−0.93 GJ/t_{CO2}) than with MEA 30 wt.% as solvent. The consumption of the liquid pumps (E_{pumps}) is similar as for MEA 30 wt.%.

Moreover, the CO_2 loading values for the rich ($\alpha_{CO2,rich}$) and the lean ($\alpha_{CO2,lean}$) solutions are equal respectively to 0.730 and 0.176 mol CO_2/mol PZ, which leads to a higher cyclic capacity than with MEA 30 wt.%.

Regarding the temperature profiles inside the columns they are quite similar to the ones obtained with MEA 30 wt.% even if for the stripper, due to the pressure level, the temperature reaches 161 °C at the bottom.

Table 8 presents the gaseous compositions of the gas treated and the produced CO_2.

Note that as indicated for MEA 30 wt.%, thanks to a water wash section (not simulated in the present case), the PZ quantity into the treated gas will be lower in the real installation.

In order to consider a stripper pressure ensuring the optimal regeneration temperature of 150 °C, the simulation results with PZ considering a regeneration pressure of 600 kPa will be taken for the comparison of configurations and solvents.

Table 7
Simulation results for the base case with PZ 40 wt.% ($(L/G)_{vol.}$ = 3.16 10^{-3}, P_{boiler} = 600 kPa).

Parameter	Value
E_{regen}	3.14 GJ/t_{CO2}
$E_{condenser}$	−0.93 GJ/t_{CO2}
E_{pumps}	1.56 10^{-2} GJ/t_{CO2}
$\alpha_{CO2,rich}$	0.730 mol CO_2/mol PZ
$\alpha_{CO2,lean}$	0.176 mol CO_2/mol PZ

Table 8
Gaseous compositions in mol. fraction for the base case with PZ 40 wt.% ($(L/G)_{vol.}$ = 3.16 10^{-3}).

Component	Gas treated	Produced CO_2
N_2	59.1%	74 ppm
CO_2	2.0%	98.0%
H_2O	30.8%	2.0%
O_2	7.8%	18 ppm
CO	0.1%	0.2 ppm
SO_2	78 ppm	145 ppm
NO	433 ppm	3 ppm
NO_2	0.7 ppm	5 ppm
PZ	790 ppm	trace

3.3. Conventional configuration with PZ-MDEA blend

3.3.1. Simulation results for different PZ-MDEA concentrations

As indicated previously, in order to make realistic comparisons with the other solvents and especially with PZ, the simulations were carried out with the same design and operating parameters as for PZ 40 wt.% (regeneration pressure fixed at 600 kPa and the total amine concentration limited to 40 wt.%). The first simulations concerned the variation of the PZ and MDEA proportions in water.

The simulation results presented on Fig. 12 were obtained for different PZ/MDEA proportions in terms of E_{regen} as a function of the $(L/G)_{vol.}$ The results for two PZ solutions (PZ 30 and 40 wt.%) are also indicated.

Globally, it can be noticed that E_{regen} for the optimum $(L/G)_{vol.}$ value is lower with the different MDEA + PZ blends in comparison with PZ alone (30 and 40 wt.%). More precisely, the blends minimizing E_{regen} were composed of 5–10 wt.% MDEA and 35–30 wt.% PZ (higher concentrations of MDEA are not favourable, certainly due to the positive effect of PZ on the absorption kinetics).

The minimum of E_{regen}, namely 2.75 GJ/t_{CO2}, was obtained with the blend composed of MDEA 10 wt.% and PZ 30 wt.% for a $(L/G)_{vol.}$ of 3.04 10^{-3} (L = 12 m^3/h). Therefore, this blend was selected for the results comparison. Note that even if validating the Aspen Hysys model with experimental values for such proportions is not yet possible, it must be reminded that the blend itself (MDEA + PZ) corresponds to a commercial solvent named aMDEA™ (©BASF) which has been already used at industrial scale and successfully simulated with Aspen software.

3.3.2. Detailed simulation results for MDEA 10 wt.% − PZ 30 wt.% blend

For the optimum value of $(L/G)_{vol.}$ (namely 3.04 10^{-3}), the detailed results are given in Tables 9 and 10.

The temperature profiles inside the columns are quite similar as the ones obtained for MEA and PZ, the temperature at the bottom of the stripper being equal to 154 °C due to the pressure level. The CO_2 loadings and the cyclic capacity of the MDEA 10 wt.% + PZ 30 wt.% blend are also similar to the ones obtained with PZ 40 wt.%, the condenser cooling energy being also reduced in comparison with PZ 40 wt.%. No major differences can be pointed out in terms of gaseous compositions.

Table 9
Simulation results for the base case with MDEA 10 wt.% + PZ 30 wt.% ($(L/G)_{vol.}$ = 3.04 10^{-3}).

Parameter	Value
E_{regen}	2.75 GJ/t_{CO2}
$E_{condenser}$	−0.59 GJ/t_{CO2}
E_{pumps}	1.58 10^{-2} GJ/t_{CO2}
$\alpha_{CO2,rich}$	0.783 mol CO_2/mol amine
$\alpha_{CO2,lean}$	0.171 mol CO_2/mol amine

Table 10
Gaseous compositions in mol. fraction for the base case with MDEA 10 wt.% + PZ 30 wt.% ($(L/G)_{vol.}$ = 3.04 10^{-3}).

Component	Gas treated	Produced CO_2
N_2	58.6%	70 ppm
CO_2	1.9%	98.0%
H_2O	31.5%	2.0%
O_2	7.7%	17 ppm
CO	0.1%	0.2 ppm
SO_2	83 ppm	103 ppm
NO	429 ppm	2.5 ppm
NO_2	1 ppm	3.5 ppm
PZ	314 ppm	trace
MDEA	2.5 ppm	trace

4. Simulation results obtained with the alternative process configurations

In addition to the operating parameters optimized for the base case (conventional process configuration), Table 11 presents the parameters that had to be optimized specifically for each process configuration.

It can be observed that Rich Solvent Recycle (RSR) and Solvent Split Flow (SSF) configurations have the highest number of parameters to be optimized (4 parameters), while the conventional configuration and Lean/Rich Vapor Compression (L/RVC) have only two parameters to be optimized. For each process configuration, the parameters were varied separately in a first step, and cross variations were carried out in a second step in order to really identify the operating conditions minimizing the solvent regeneration duty, which is challenging.

4.1. Rich Solvent Recycle (RSR) configuration

First of all, the influence of the re-injected solution temperature on the process performances was investigated and is illustrated on Fig. 13 for MEA 30 wt.%, considering a liquid flow rate of 24 m^3/h and 35% of solution re-injection into the stripper at stage 4. The effect of cooling the re-injected solution is presented in terms of regeneration energy and rich CO_2 loading.

As expected by an absorption enhancement process modification as RSR, the recirculation into the absorber of a cooled solution allows to increase the CO_2 loading of the rich solution (from 0.50 to 0.51 mol CO_2/mol MEA in the presented case when the solution is cooled from 50 °C to 5 °C) which leads to a decrease of the regeneration energy from

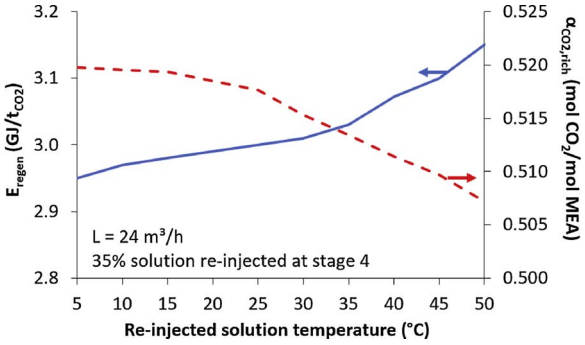

Fig. 13. E_{regen} and $\alpha_{CO2,rich}$ as a function of the re-injected solution temperature into the absorber (35% re-injection at stage 4) – RSR configuration with MEA 30 wt.%.

3.30 to 3.12 GJ/t_{CO2}. Nevertheless, cooling the solution to a too low level would be unfavorable in terms of cooling energy. In practice, considering a cooling of the solution from ≈60 °C (temperature of the solution at the outlet of the absorber) to 40 °C (same temperature of the solution at the top of the absorber) seems more feasible on a practical point of view and will be considered as reference for the results comparison between the different solvents and configurations. It must be noted that in practice, if more cooling energy is available for decreasing the recirculated solvent temperature, that will allow a reduction of the maximum solvent temperature inside the column (see temperature profile on Fig. 7(a)) which will still be favourable in terms of absorption kinetics.

For each solvent, the simulation results considering RSR configuration are presented on Figs. 14–16 illustrating the optimization of the different operating parameters, namely $(L/G)_{vol.}$, the fraction of the cold solution re-injected into the absorber ("split fraction") and the re-injection stage of the rich solution after cooling. Note that for each graph, the optimum values of the other parameters were considered.

Globally, it can be observed that the lowest values of E_{regen} were obtained with the blend composed of MDEA and PZ, while MEA and PZ give quite similar results. The influence of $(L/G)_{vol.}$ on E_{regen} is identical for all the solvents even if due to the difference in terms of solvent physico-chemical properties and absorption capacities, the $(L/G)_{vol.}$ ranges are different from a solvent to another one, the optimum value of $(L/G)_{vol.}$ being higher with MEA 30 wt.% (6.06 10^{-3}) than with PZ 40 wt.% (3.54 10^{-3}) and MDEA 10 wt.% + PZ 30 wt.% (3.04 10^{-3}). Regarding the influence of the two other parameters (split fraction and re-injection stage of the cold rich solution), it is more pronounced with MEA 30 wt.% than with the other solvents but in each case, it was possible to identify the value parameter minimizing E_{regen}.

The simulation results obtained with each solvent considering RSR configuration are globally compared and discussed in Section 4.5.

4.2. Solvent Split Flow (SSF) configuration

Three operating parameters must be optimized with the "Solvent Split Flow" (SSF) configuration, namely the $(L/G)_{vol.}$ (as for all the configurations), the fraction of the rich solution ("cold fraction") which

Table 11
Parameters optimized for each process configuration.

Type of variable	Conventional	RSR	SSF	LVC	RVC
Flow rate ratio	$(L/G)_{vol.}$	$(L/G)_{vol.}$	$(L/G)_{vol.}$	$(L/G)_{vol.}$	$(L/G)_{vol.}$
Level	Injection level into the stripper	Re-injection level into the absorber	Injections level of the cold solution into the stripper Injections level of the preheated solution into the stripper	–	–
Temperature	–	Re-injection temperature into the absorber		–	–
Flow fraction	–	Re-injected fraction	Split fraction	–	–
Pressure	–	–	–	Flash pressure	Flash pressure

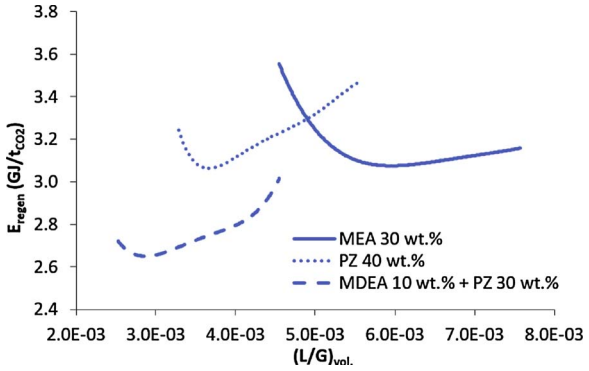

Fig. 14. E_{regen} as a function of the $(L/G)_{vol.}$ for the different solvents and considering the optimum split fraction and injection stage – RSR configuration.

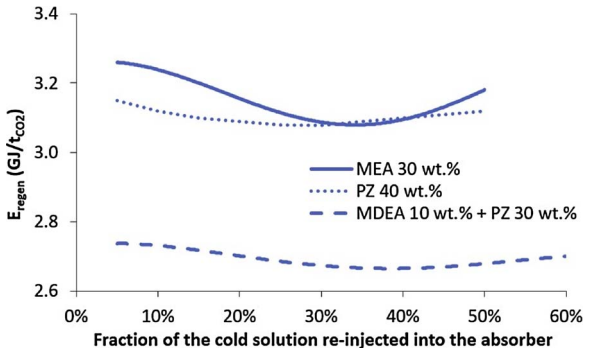

Fig. 15. E_{regen} as a function of the percentage of re-injected solution into the absorber for the different solvents and considering the optimum $(L/G)_{vol.}$ and injection stage – RSR configuration.

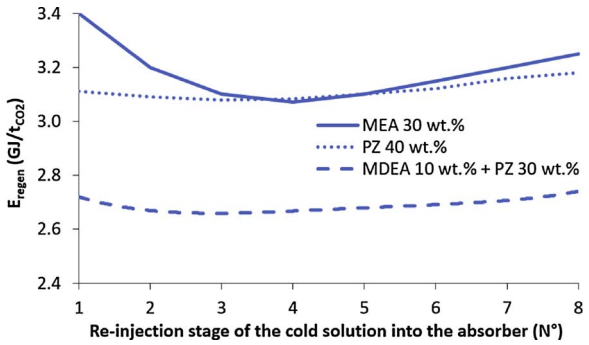

Fig. 16. E_{regen} as a function of the re-injection stage of the cold rich solution into the absorber for the different solvents and considering the optimum $(L/G)_{vol.}$ and split fraction – RSR configuration.

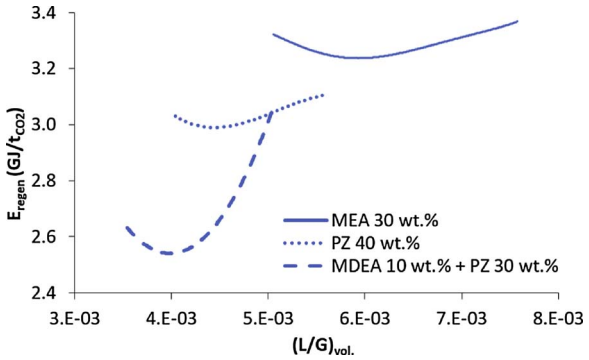

Fig. 17. E_{regen} as a function of the $(L/G)_{vol.}$ for the different solvents and considering the optimum cold fraction and injection stage – SSF configuration.

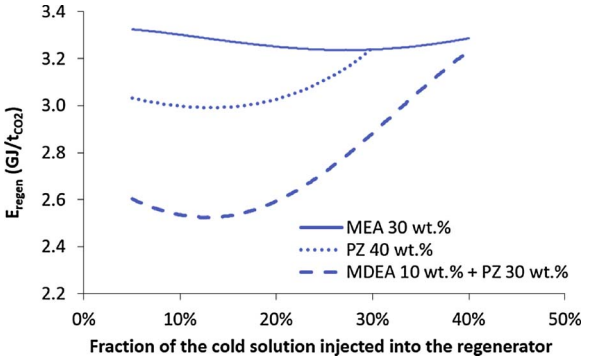

Fig. 18. E_{regen} as a function of the percentage of re-injected solution into the regenerator for the different solvents and considering the optimum $(L/G)_{vol.}$ and injection stage – SSF configuration.

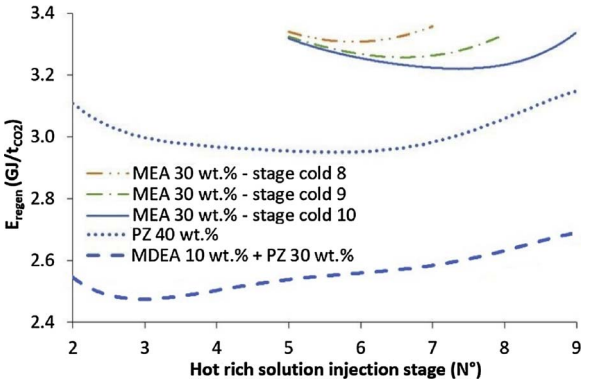

Fig. 19. E_{regen} as a function of the re-injection stage of the hot rich solution into the regenerator for the different solvents and considering the optimum $(L/G)_{vol.}$ and cold fraction (different cold fractions for MEA) – SSF configuration.

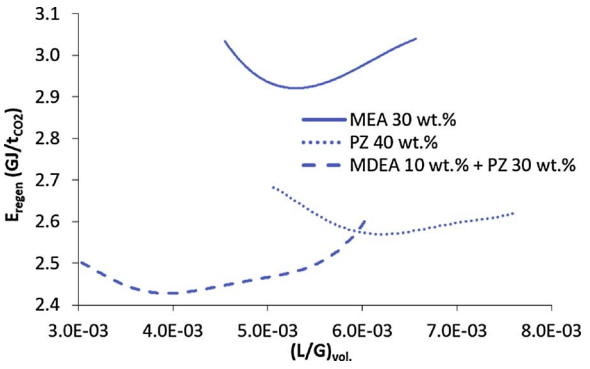

Fig. 20. E_{regen} as function of the $(L/G)_{vol.}$ ratio for the optimum value of Δp for each solvent – LVC configuration.

is injected without being preheated and the re-injection level of the preheated solution into the regeneration column. Regarding the cold solution, it is conventionally injected at the top of the stripper (stage 10 in a first step) in order to reduce the condenser cooling energy.

For each solvent, the simulation results considering SSF configuration are presented on Figs. 17–19.

Regarding the results presented on Fig. 17, as for the previous configurations, it can be seen that the optimum liquid flow rate ($(L/G)_{vol.}$ minimizing E_{regen}) is lower with MDEA + PZ solution than with PZ and MEA. Concerning the influence of the cold fraction, as illustrated on Fig. 18, it is more pronounced with PZ-based solvents than with MEA, the fraction of the cold solution minimizing E_{regen} being in the range 15% to 30% depending of the solvent. Finally, considering for each solvent the optimum liquid flow rate and split fraction, Fig. 19

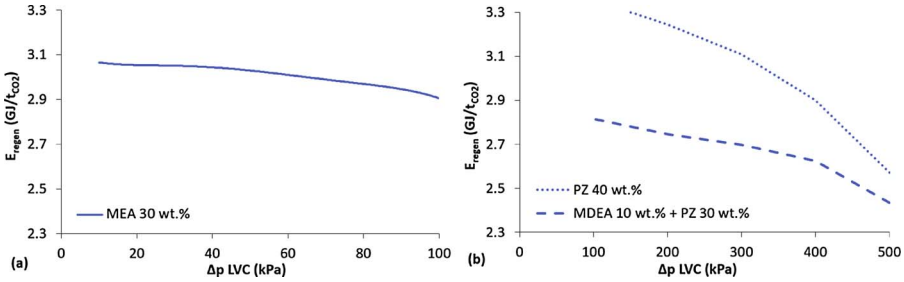

Fig. 21. E_{regen} as function of the Δp LVC for MEA 30 wt.% (a), PZ 40 wt.% and MDEA 10 wt.% + PZ 30 wt.% (b) for the optimum $(L/G)_{vol.}$ ratio – LVC configuration.

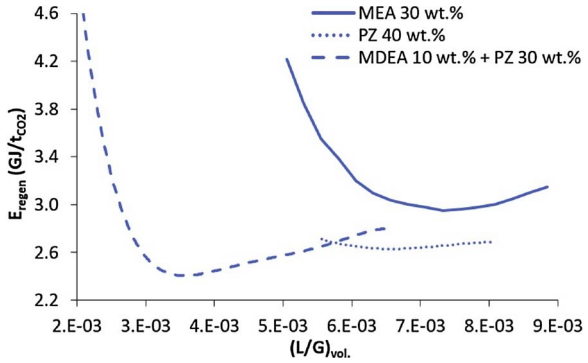

Fig. 22. E_{regen} as function of the $(L/G)_{vol.}$ ratio for the optimum value of Δp for each solvent – RVC configuration.

shows the influence of the injection stage of the hot and cold rich solutions into the stripper. As illustrated for MEA 30 wt.% (the same observation was made for the other solvents), the best results were obtained when the cold solution is injected at the top of the stripper (stage 10). Regarding the optimum hot solution injection stage, it was identified at stage 6 and 7 for PZ 40 wt.% and MEA 30 wt.% respectively, while the minimum of E_{regen} was obtained when this solution was injected at stage 3 for the blend MDEA 10 wt.% + PZ 30 wt.%.

The details and the discussions in relation with the simulation results obtained with each solvent considering SSF configuration are available in Section 4.5.

4.3. Lean Vapor Compression (LVC) configuration

In addition to the $(L/G)_{vol.}$ (as for all the other configurations, especially the liquid flow rate, the gaseous flow rate being fixed), the important operating parameter regarding the LVC configuration is the flash pressure variation (Δp from 0 to 100 kPa for MEA and from 0 to 500 kPa for PZ-based solvents). It must be also reminded that this process modification is generally accompanied with an expansion (or a modification) of the internal heat exchanger in order to reduce the hot pinch of this exchanger to 5 °C and that another heat exchanger cools down the LVC flash vapor to 120 °C in order to avoid any hot spot leading to solvent and material degradations. The simulation results for each solvent considering LVC configuration are presented on Figs. 20 and 21.

Regarding the results presented on Fig. 20, the main observation is similar as with the other configurations, namely the value of $(L/G)_{vol.}$ minimizing E_{regen} is lower for the MDEA 10 wt.% + PZ 30 wt.% solvent than with other solvents. Nevertheless, in the present case the optimum $(L/G)_{vol.}$ value with PZ 40 wt.% (namely 6.07 10^{-3}) is a little bit higher than with MEA 30 wt.% (namely 5.30 10^{-3}).

Concerning the influence of the LVC flash pressure variation (Δp), Fig. 21(a) for MEA 30 wt.% and Fig. 21(b) for PZ-based solvents highlight that despite the decrease of the temperature of the rich solution at the outlet of the internal heat exchanger (for example, a decrease of almost 20 °C was observed with MEA 30 wt.% in comparison with the conventional configuration), a higher LVC flash pressure variation leads to a quasi linear decrease of the regeneration energy.

This effect was observed for both solvents even if it is more pronounced with PZ-based solvents than with MEA 30 wt.% due to the fact that these solvents were regenerated at a higher pressure (600 kPa) than MEA 30 wt.% (200 kPa) allowing a larger Δp. Note that even if due to the flash operation the temperature of the rich solution at the outlet of the internal heat exchanger is decreased, another heat exchanger gives a complementary preheating to the rich solution (from 2 to 5 °C) thanks to its heat exchange with the hot vapor coming from the LVC unit.

Other simulation results (such as CO_2 loadings) and energy consumptions (pumps and LVC-compressor), are presented and discussed in Section 4.5.

4.4. Rich Vapor Compression (RVC) configuration

As for the LVC configuration, in addition to the $(L/G)_{vol.}$, the important operating parameter regarding the RVC configuration is the flash pressure variation (Δp from 0 to 100 kPa for MEA and from 0 to 500 kPa for PZ-based solvents). A supplementary heat exchanger also cools down the RVC flash vapor to 120 °C in order to avoid any hot spot in the stripper.

The simulation results for each solvent considering RVC configuration are presented on Figs. 22 and 23.

As presented on Fig. 22, the influence of $(L/G)_{vol.}$ on E_{regen} leads to the same observations as with the other configurations, namely the value of this ratio minimizing the regeneration energy is lower with MDEA 10 wt.% + PZ 30 wt.% than with the other solvents, especially MEA 30 wt.%. The effect of the RVC flash pressure variation (Δp) illustrated on Fig. 23(a) for MEA 30 wt.% and Fig. 23(b) for PZ-based

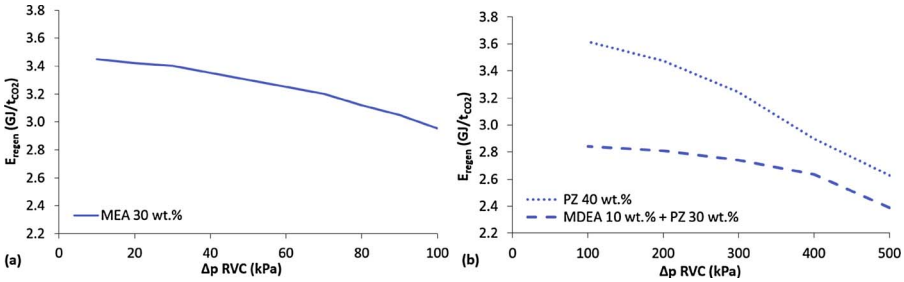

Fig. 23. E_{regen} as function of the Δp RVC for MEA 30 wt.% (a), PZ 40 wt.% and MDEA 10 wt.% + PZ 30 wt.% (b) for the optimum $(L/G)_{vol.}$ ratio − RVC configuration.

Table 12
Summary of the simulation results for the different configurations with the three solvents considered (optimum operating conditions).

	Conventional configuration			RSR configuration			SSF configuration			LVC configuration			RVC configuration		
	MEA	PZ	MDEA + PZ	MEA	PZ	MDEA + PZ	MEA	PZ	MDEA + PZ	MEA	PZ	MDEA + PZ	MEA	PZ	MDEA + PZ
Operating conditions															
$(L/G)_{vol,opt}$ (m^3/m^3)	$5.56\ 10^{-3}$	$3.16\ 10^{-3}$	$3.04\ 10^{-3}$	$6.06\ 10^{-3}$	3.5410^{-3}	$3.04\ 10^{-3}$	$5.81\ 10^{-3}$	$4.55\ 10^{-3}$	$4.03\ 10^{-3}$	$5.30\ 10^{-3}$	$6.07\ 10^{-3}$	$3.54\ 10^{-3}$	$7.33\ 10^{-3}$	$6.57\ 10^{-3}$	$3.54\ 10^{-3}$
Split fraction rich sol. (%)	–	–	–	35	30	40	26	15	15	–	–	–	–	–	–
Re-injection sol. temp. (°C)	–	–	–	40	40	40	–	–	–	–	–	–	–	–	–
Re-injection abs. stage (N°)	–	–	–	4	3	3	–	–	–	–	–	–	–	–	–
Hot sol. stripper stage (N°)	–	–	–	–	–	–	7	6	3	–	–	–	–	–	–
Cold sol. stripper stage (N°)	–	–	–	–	–	–	10	10	10	–	–	–	–	–	–
Flash Δp (kPa)	–	–	–	–	–	–	–	–	–	100	500	500	100	500	500
$\alpha_{CO2,rich}$ (mol/mol)	0.51	0.73	0.78	0.51	0.71	0.79	0.50	0.70	0.72	0.51	0.67	0.74	0.47	0.53	0.75
$\alpha_{CO2,lean}$ (mol/mol)	0.21	0.18	0.17	0.24	0.23	0.17	0.22	0.33	0.26	0.20	0.45	0.27	0.25	0.27	0.27
Energy consumptions															
E_{pump} (GJ/t_{CO2})	$1.57\ 10^{-2}$	$1.56\ 10^{-2}$	$1.58\ 10^{-2}$	$1.57\ 10^{-2}$	$1.58\ 10^{-2}$	$1.56\ 10^{-2}$	$1.57\ 10^{-2}$	$1.57\ 10^{-2}$	$1.57\ 10^{-2}$	$1.58\ 10^{-2}$	$2.67\ 10^{-2}$	$2.19\ 10^{-2}$	$1.58\ 10^{-2}$	$2.70\ 10^{-2}$	$2.15\ 10^{-2}$
E_{cooler} (-GJ/t_{CO2})	1.51	0.03	0.02	1.42	0.03	0.02	1.64	0.43	0.55	1.04	1.19	0.30	2.36	2.04	0.24
$E_{condenser}$ (-GJ/t_{CO2})	1.94	0.93	0.59	1.89	1.04	0.64	1.02	0.49	0.23	0.91	0.82	0.60	1.52	0.73	0.48
$E_{LVC/RVC,compressor}$ (GJ/t_{CO2})	–	–	–	–	–	–	–	–	–	$8.28\ 10^{-2}$	$65\ 10^{-2}$	$37\ 10^{-2}$	$13.6\ 10^{-2}$	$65\ 10^{-2}$	$29\ 10^{-2}$
E_{regen} (GJ/t_{CO2})	3.36	3.14	2.75	3.07	3.08	2.66	3.22	2.99	2.49	2.91	2.57	2.43	2.95	2.63	2.39
W_{equ} (GJ/t_{CO2})	0.59	0.71	0.60	0.54	0.69	0.58	0.56	0.67	0.54	0.59	1.24	0.91	0.65	1.26	0.82
$C_{utilities}$ [a] (€/t_{CO2})	33.54	33.08	28.29	30.07	32.81	30.07	25.82	29.06	28.52	28.32	39.11	32.06	30.87	32.21	30.87

[a] Currency conversion in October 2017: 1 US $ is equal to 0.8505 €.

solvents is similar as for the LVC configuration, a higher Δp being preferred in order to minimize the regeneration energy.

The other energy consumptions (pumps and RVC-compressor) as well as simulation results are globally discussed in Section 4.5.

4.5. Summary of the simulations results obtained with the different configurations and solvents

4.5.1. Global comparison of the energy savings thanks to different process configurations

For the optimum value of $(L/G)_{vol.}$ (namely $3.04\ 10^{-3}$), the detailed results are given in Tables 9 and 10.

A summary of the optimal operating conditions and corresponding simulations results for each configuration and solvent is provided in Table 12. Regarding the CO_2 loading values of the rich and lean solutions (illustrated on Fig. 24(a) and (b) respectively), it can be seen that for all the solvents, the process configuration does not lead to a significant modification of the rich solution CO_2 loading, except for PZ 40 wt.% applying RVC configuration, its rich CO_2 loading being reduced from 0.73 mol CO_2/mol PZ (conventional process) to 0.53 mol CO_2/mol PZ (with RVC). This observation is justified by the fact that the optimum $(L/G)_{vol.}$ in such case is higher than with other configurations, leading to a decrease of the CO_2 cyclic capacity and thus of the rich CO_2 loading (the CO_2 absorption rate being kept at 90%). Comparing the different solvents, PZ-based solutions have higher rich CO_2 loadings (up to almost 0.8 mol CO_2/mol amine) that MEA 30 wt.% (around 0.5 mol CO_2/mol amine). Concerning the lean CO_2 loading values, the main observation is the fact that quite logically, thanks to alternative configurations, the solutions can be less regenerated (higher $\alpha_{CO2,lean}$ values) leading to a decrease of the regeneration duty. Note that in the case of PZ 40 wt.% applying the LVC configuration, the $\alpha_{CO2,lean}$ is particularly high (0.45 mol CO_2/mol PZ) in comparison with other solvents.

Focusing now on the energy consumptions, it can be seen in Table 12 that the pumping energy (E_{pump}) is very low (from $1.5\ 10^{-2}$ to $2.7\ 10^{-2}$ GJ/t_{CO2}) in comparison with the other energy demands. Even if it is more significant (from $8\ 10^{-2}$ to $65\ 10^{-2}$ GJ/t_{CO2}) than E_{pump}, the energy used for compression in LVC and RVC configurations is clearly lower than the solvent regeneration energy (from 2 to 3 GJ/t_{CO2}). Note that a real comparison between these energy consumptions is not allowed due to the fact that pumping and compression use electrical energy while regeneration needs thermal energy. Regarding the compression energy, naturally, $E_{LVC/RVC,compressor}$ is higher with PZ-based solvents due to the operating regeneration pressure (600 kPa) allowing a higher Δp (500 kPa) than with MEA 30 wt.% (100 kPa).

Nevertheless, as shown by (Fernandez et al., 2012) for the case of MEA and LVC configuration, the economic interest of such configuration is confirmed even if it implies the use of a compressor. Moreover, this type of configuration is also successfully in operation in several industrial plants using commercial solvents (e.g. Boundary Dam plant at Saskatchewan, Canada) and inducing different operating conditions than with MEA.

Concerning the condenser and cooler cooling energies ($E_{condenser}$ and E_{cooler}) presented in Table 12 and on Fig. 25(a) and (b), the first observation is that for almost all the simulation cases, the cooling demands are lower with PZ-based solvents than with MEA 30 wt.%.

The condenser cooling demand is significantly reduced with the use of the other process configurations, especially with the SSF one using PZ-based solvents (< 0.5 GJ/t_{CO2}). Regarding the cooling demand for keeping the lean solvent temperature at 40 °C before entering the absorber (E_{cooler}), it is higher with PZ-based solvents and LVC/RVC configurations than with conventional one. Nevertheless, in the case of MEA 10 wt.% + PZ 30 wt.% blend and for each configuration except SSF one, E_{cooler} is always significantly lower than $E_{condenser}$ (e.g. E_{cooler} corresponds to 50% of $E_{condenser}$ for both LVC and RVC configurations using this blend as solvent).

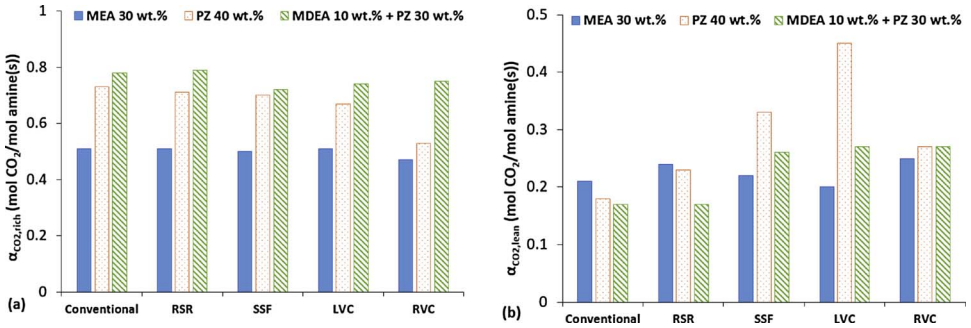

Fig. 24. CO_2 loading values of the rich (a) and lean (b) solutions for the different solvents and process configurations.

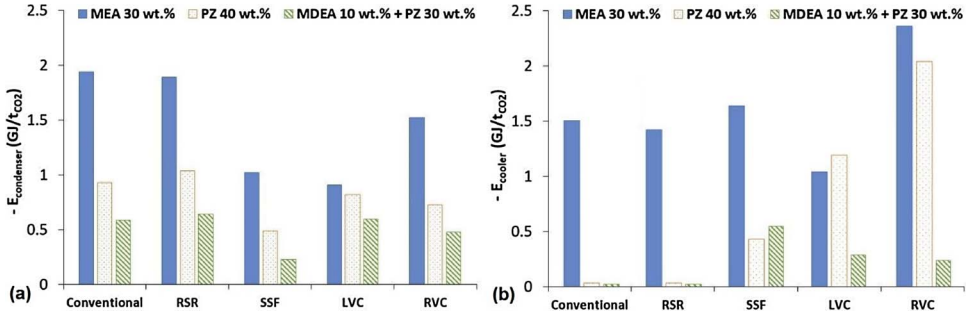

Fig. 25. $E_{condenser}$ (a) and E_{cooler} (b) corresponding to the optimal operating conditions as a function of the configuration for the three solvents considered.

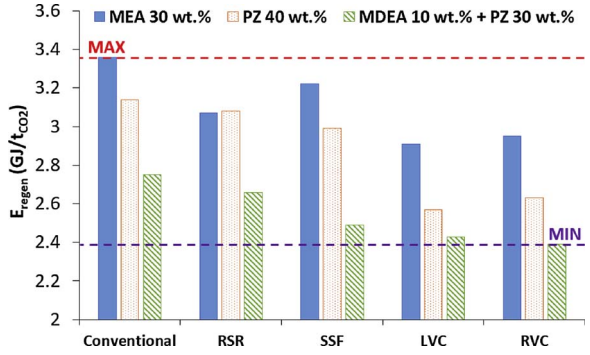

Fig. 26. Optimum value of E_{regen} as a function of the configuration for the three solvents considered.

4.5.2. Comparison of the solvents and configurations based on the regeneration energy and effect of y_{CO2}

Fig. 26 compares the values of the regeneration energy obtained with the different solvents and process configurations for the inlet CO_2 content of 20%.

It is confirmed that for all the solvents, the LVC and RVC configurations (heat pumps modifications) lead to the higher energy savings in comparison with the conventional configuration, the specific regeneration energy of all the solvents using LVC or RVC configurations becoming lower than 3 GJ/t_{CO2}, which is clearly a relevant result. Indeed, obtaining such a low regeneration energy with MEA 30 wt.% is not conventional and it can be partially linked to the fact that the flue gas considered in the present study (coming from a cement plant) contains more CO_2 (y_{CO2} equal to 20 vol.%) than for a power plant (y_{CO2} from 5 vol.% to 15 vol.%) considered in most of other studies. The interest of higher y_{CO2} values is specifically discussed in another paper (Dubois et al., 2017) considering the conventional configuration with MEA 30 wt.% (experimental and simulation results) and also with other solvents (experimental absorption-regeneration results with conventional process configuration). The simulation results presented in (Dubois et al., 2017) were completed on Fig. 27 with simulation results obtained for the different process configurations with MEA 30 wt.% and for an identical amount of CO_2 captured (namely 1.5 t_{CO2}/h, which corresponds to an absorption ratio of 90% at y_{CO2} equal to 20 mol%). For each case and $y_{CO2,in}$ value, the liquid flow rate was adjusted in order to minimize E_{regen}.

It can be pointed out from Fig. 27 that for a higher CO_2 content in the gas to treat (from 20 mol% to 60 mol%), E_{regen} is reduced for all the

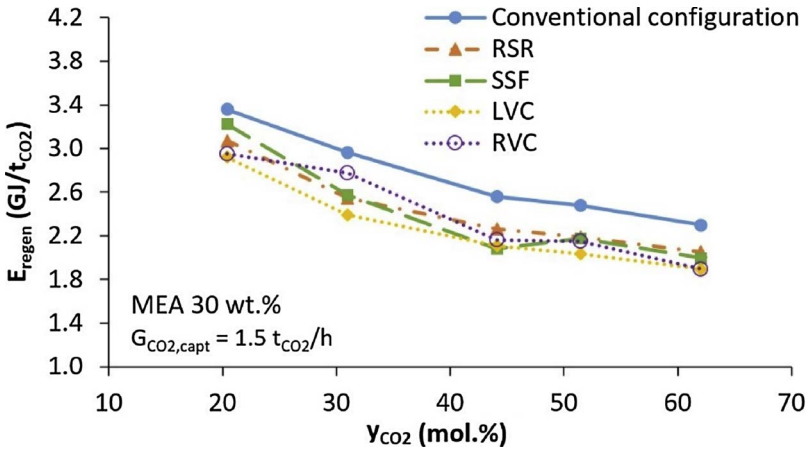

Fig. 27. E_{regen} as a function of the inlet CO_2 content for the different configurations with MEA 30 wt.%.

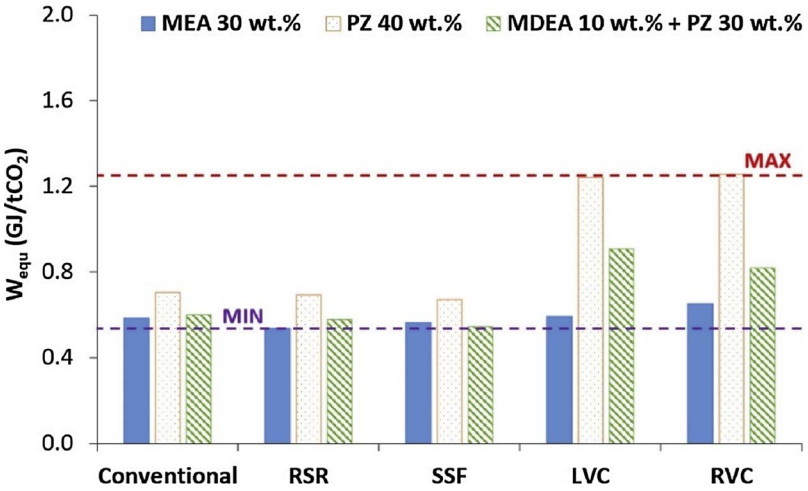

Fig. 28. W_{equ} as a function of the configuration for the three solvents considered.

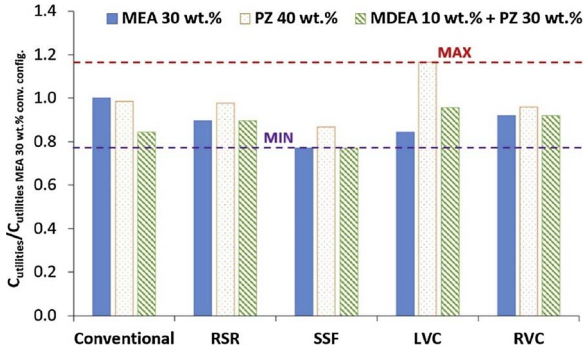

Fig. 29. $C_{utilities}$ relatively to conventional configuration with MEA 30 wt.% as a function of the configuration for the three solvents considered.

configurations considered. This effect is also present with other solvents and it will be more deeply investigated in a forthcoming paper.

Regarding the comparison of the solvents on Fig. 26, it appears that PZ 40 wt.% and MDEA 10 wt.% + PZ 30 wt.% lead to a lower regeneration energy in comparison with the benchmark MEA 30 wt.%. More precisely, it was shown that there is an interest of replacing 10 wt.% of PZ by 10 wt.% of MDEA. The lowest regeneration energy was obtained with MDEA 10 wt.% + PZ 30 wt.% applying RVC configuration, namely 2.39 GJ/t_{CO2}.

4.5.3. Comparison of the solvents and configurations based on the equivalent work

Fig. 28 compares the values of the total thermodynamic equivalent work obtained with the different solvents and process configurations. It can be seen that due to the higher regeneration temperature with PZ-based solvents (150 or 160 °C) in comparison with MEA 30 wt.% (120 °C), and due to electrical consumption of LVC or RVC compressors, the solvent and configuration combinations that minimize W_{equ} (e.g. MEA 30 wt.% applying RSR configuration or MDEA 10 wt.% + PZ 30 wt.% applying SSF configuration) do not correspond to the ones minimizing E_{regen} (e.g. MDEA 10 wt.% + PZ 30 wt.% applying RVC configuration). This difference can be explained by the fact that the operating parameters were specifically adjusted in order to minimize E_{regen} and not W_{equ}, which means that other operating parameters could lead to lower W_{equ} values. Nevertheless, the approach of minimizing E_{regen} instead of W_{equ} in the case of a cement plant can be justified by the fact that, on the contrary to a power plant (where it is common to quantify the efficiency loss on the plant, and thus directly taking into account the needed electrical consumption), the electrical consumption linked to devices (e.g. pumps or compressors) will come from an external source, which could be a renewable one or corresponds to excess power production.

Moreover, it must be pointed out that even if it is not taken into account in the present work, some thermal energy could be recovered into a cement plant (from 5% to 15% of E_{regen} depending on the plant). Thus, the need of external energy (electricity) could be partially counterbalanced by less steam needed for the solvent regeneration.

4.5.4. Comparison of the solvents and configurations based on the utilities cost

Finally, Fig. 29 compares the values of the utilities costs obtained with the different solvents and process configurations.

The $C_{utilities}$ values on Fig. 29 are reported to MEA 30 wt.% with the conventional configuration in order to perform a relative comparison. Indeed, the utilities calculations made by Aspen Economics module in Aspen Hysys consider some hypotheses in order to perform the cost calculations and the $C_{utilities}$ values themselves (indicated in Table 12) should be considered carefully. Nevertheless, as the calculation method and hypotheses were similar for all the cases, a relative comparison can be considered as an interesting indication to perform an analysis between the different solvents and configurations.

As for the comparison based on E_{regen} or W_{equ}, it can be seen from Fig. 29 that several combinations of solvent and configuration (e.g. MEA 30 wt.% or MDEA 10 wt.% + PZ 30 wt.% with SSF configuration) lead to better results (lower costs in the present case) than MEA 30 wt.% ones using the conventional configuration. On the contrary to W_{equ}, two observations can be drawn, namely: the utilities costs with all the solvents implementing RVC configuration are lower than MEA 30 wt.% ones using the conventional configuration, and all the utilities costs with MDEA 10 wt.% + PZ 30 wt.% solvent are lower than MEA 30 wt.% ones.

5. Conclusions and perspectives

In the context of reducing the CO_2 emissions from cement plants, and in order to reduce the CO_2 capture costs specifically for the application in the cement industry, the present study focused on the Aspen Hysys™ simulation of different configurations of the absorption-regeneration CO_2 capture process using amine based solvents (MEA 30 wt.%, PZ 40 wt.% and MDEA 10 wt.% + PZ 30 wt.%) and applied to the flue gas coming from the Norcem Brevik Cement plant in Norway (considered as case study). The design of the CO_2 capture plant considered for the simulation was based on the CASTOR/CESAR European Projects pilot. Four process modifications were investigated, namely RSR, SSF, LVC and RVC, in order to be representative of the three categories of process modifications: absorption enhancement, exergetic or heat integration and heat pump effect respectively. For each configuration, a systematic parametric study on operating parameters ($(L/G)_{vol.}$, split ratios, flash pressure variations, etc.)

was carried out aiming at identifying the conditions minimizing the regeneration energy (taken as main comparison factor for each configuration). The total equivalent thermodynamic work and the utilities costs were also analyzed in order to compare different configuration and solvent combinations.

Based on the simulations carried out, it was pointed out that the heat pump modifications LVC and RVC lead to the higher regeneration energy savings (from 11% to 18% depending on the solvent) while also reducing significantly the condenser cooling energy. The energy savings linked to RSR and SSF modifications were lower (between 2% and 10%). Regarding the comparisons of the solvents, the best results in terms of regeneration energy were obtained with the blend MDEA 10 wt.% + PZ 30 wt.% applying RVC configuration and leading to a regeneration energy equal to 2.39 GJ/t_{CO2}. The lower regeneration energies obtained in the present study were partially related to the interest of treating a rich-CO_2 flue gas, which is the case with cement plant flue gases. Regarding the comparisons based on total equivalent work and utilities costs, it was shown that the cases (solvent + configuration) minimizing E_{regen} does not correspond to the cases minimizing W_{equ} and/or $C_{utilities}$. Nevertheless, regardless the approach considered, it was confirmed that implementing alternative process configurations and other solvents than MEA 30 wt.% leads to lower energy consumptions or costs. Moreover, in the case of a cement plant, thermal energy could be recovered directly in the plant and all the electrical consumptions will come from an external source without influencing the cement plant performances itself, which justifies the approach considered in the present work, namely minimizing the solvent regeneration energy.

As perspectives, other configurations will be also investigated such as the combination of two configurations (for example RSR and RVC, or the combination of RVC/LVC with an Intercooled Absorber (ICA)). Exergy analyzes and life cycle assessment (LCA) will be also envisaged as criterion for the optimization of the operating parameters considering different solvents and process configurations. Finally, in addition to the interest in terms of regeneration energy and OPEX, the consequence in terms of CAPEX will be estimated for a more precise evaluation of the global economic interest of using alternative process configurations for the application of the post-combustion CO_2 capture in the cement industry.

Acknowledgments

The authors would like to acknowledge the European Cement Research Academy (ECRA) and HeidelbergCement Company for their technical and financial support accorded to the ECRA Academic Chair at the University of Mons.

References

Bjerge, L.-M., Brevik, P., 2014. CO_2 capture in the cement industry, Norcem CO_2 capture project (Norway). Energy Procedia 63, 6455–6463.
Dubois, L., Laribi, S., Mouhoubi, S., De Weireld, G., Thomas, D., 2017. Study of the post-combustion CO_2 capture applied to conventional and partial oxy-fuel cement plants. Energy Procedia 114, 6181–6196.
Fernandez, E.S., Bergsma, E.J., Mercader, F., Goetheer, E.L.V., Vlugt, T.J.H., 2012. Optimisation of lean vapour compression (LVC) as an option for post-combustion CO2 capture: net present value maximization. Int. J. Greenhouse Gas Control S114–S121.
Ferrara, G., Lanzini, A., Leone, P., Ho, M.T., Wiley, D.E., 2017. Exergetic and exergoeconomic analysis of post-combustion CO_2 capture using MEA-solvent chemical absorption. Energy 130, 113–128.
Freeman, S.A., Dugas, R., Van Wagener, D.H., Nguyen, T., Rochelle, G.T., 2010. Carbon dioxide capture with concentrated, aqueous piperazine. Int. J. Greenhouse Gas Control 4, 119–124.
Gervasi, J., Dubois, L., Thomas, D., 2014. Simulation of the post-combustion CO_2 capture with Aspen Hysys™ software: study of different configurations of an absorption-regeneration process for the application to cement flue gases. Energy Procedia 63, 1018–1028.
Idem, R., Supap, T., Shi, H., Gelowitz, D., Ball, M., Campbell, C., Tontiwachwuthikul, P., 2015. Practical experience in post-combustion CO_2 capture using reactive solvents in large pilot and demonstration plants. Int. J. Greenhouse Gas Control 40, 6–25.
IEA (International Energy Agency), 2013. Technology Roadmap Carbon Capture and Storage, 2013 edition. .
Karimi, M., Hillestad, M., Svendsen, H.F., 2011. Capital costs and energy considerations of different alternative stripper configurations for post combustion CO_2 capture. Chem. Eng. Res. Des. 89, 1229–1236.
Knudsen, J.N., Jensen, J.N., Vilhelmsen, P.-J., Biede, O., 2009. Experience with CO_2 capture from coal flue gas in pilot-scale: testing of different amine solvents. Energy Procedia 1, 783–790.
Le Moullec, Y., Neveux, T., Chikukwa, A., Hoff, A., 2014. Process modifications for solvent-based post-combustion CO_2 capture. Int. J. Greenhouse Gas Control 31, 96–112.
Mudhasakul, S., Ku, H.-M., Douglas, P.L., 2013. A simulation model of a CO_2 absorption process with methyldiethanolamine solvent and piperazine as an activator. Int. J. Greenhouse Gas Control 15, 134–141.
Roh, K., Lee, J.H., Gani, R., 2016. A methodological framework for the development of feasible CO_2 conversion processes. Int. J. Greenhouse Gas Control 47, 250–265.
Sanchez Fernandez, E., Bergsma, E.J., de Miguel Mercader, F., Goetheer, E.L.V., Vlugt, T.J.H., 2012. Optimisation of lean vapour compression (LVC) as an option for post-combustion CO2 capture: net present value maximization. Int. J. Greenhouse Gas Control S114–S121.
Singh, P., Van Swaaij, W.P.M., Brilman, D.W.F., 2013. Energy efficient solvents for CO_2 absorption from flue gas: vapor liquid equilibrium and pilot plant study. Energy Procedia 37, 2021–2046.
Song, Y., Chen, C.-C., 2009. Symmetric electrolyte nonrandom two-liquid activity coefficient model. Ind. Eng. Chem. Res. 48, 7788–7797.
van der Ham, L.V., Romano, M.C., Kvamsdal, H.M., Bonalumi, D., van Os, P., Goetheer, E.L.V., 2014. Concentrated aqueous piperazine as CO_2 capture solvent: detailed evaluation of the integration with a power plant. Energy Procedia 63, 1218–1222.
Zhang, Y., Chen, C.-C., 2011. Thermodynamic modeling for CO_2 absorption in aqueous MDEA solution with electrolyte NRTL model. Ind. Eng. Chem. Res. 50, 163–175.
Zhang, Y., Chen, H., Chen, C.-C., Plaza, J.M., Dugas, R., Rochelle, G.T., 2009. Rate-based process modeling study of CO_2 capture with aqueous monoethanolamine solution. ind. Eng. Chem. Res. 48, 9233–9246.
Zhang, Y., Que, H., Chen, C.-C., 2011. Thermodynamic modeling for CO_2 absorption in aqueous MEA solution with electrolyte NRTL model. Fluid Phase Equilib. 311, 68–76.
Zhao, X., Smith, K.H., Simioni, M.A., Tao, W., Kentish, S.E., Fei, W., Stevens, G.W., 2011. Comparison of several packings for CO2 chemical absorption in a packed column. Int. J. Greenhouse Gas Control 5, 1163–1169.